



Cite this: *Green Chem.*, 2024, **26**, 10290

## Preparation of methyl ethyl ketone from biomass-derived levulinic acid using a metal-free photocatalytic system and life cycle assessment study†

Meng-Xiang Shen, Chen-Qiang Deng, Jie Yang and Jin Deng \*

Levulinic acid (LA) is derived from lignocellulosic biomass and can undergo various chemical transformations to produce high-value chemicals. However, there are limited studies on C–C bond cleavage in LA. Methyl ethyl ketone (MEK) is a high-quality solvent with a wide range of industrial applications, traditionally produced from petroleum-derived *n*-butene. Here, we report a method for the production of MEK from LA using a metal-free photocatalytic system. Using acridine compounds as photosensitizers and thiophenols as hydrogen transfer reagents, high selectivity and yield of MEK are achieved under mild reaction conditions, and the reaction time is significantly shortened using a microchannel continuous flow photo-reactor. Additionally, life cycle assessment indicates that this method has lower carbon emissions than other MEK production methods from LA. This catalytic system provides a green and efficient method to produce MEK from bio-based platform molecule LA, which meets the requirements of sustainable development.

Received 10th June 2024,  
Accepted 4th September 2024

DOI: 10.1039/d4gc02798a

[rsc.li/greenchem](http://rsc.li/greenchem)

### Introduction

With the increasing consumption of petrochemical resources, environmental pollution and the greenhouse effect have become very serious.<sup>1</sup> It is necessary to develop substitutes for fossil resources to achieve sustainable development.<sup>2–4</sup> Biomass, as a clean and renewable energy source, has been considered the only source of organic carbon that can substitute petroleum resources.<sup>5,6</sup> The main components of lignocellulosic biomass are lignin, cellulose, and hemicellulose.<sup>7</sup> Among these, cellulose (*e.g.*, hexose-derived 5-hydroxymethylfurfural) and hemicellulose (*e.g.*, pentosan-derived furfuryl alcohol) can be catalytically hydrolyzed to produce levulinic acid (LA).<sup>8–10</sup> LA contains carbonyl and carboxyl groups, which are prone to esterification, halogenation, hydrogenation, oxidative, and condensation.<sup>11</sup> It can synthesize high-value-added chemicals such as  $\gamma$ -valerolactone (GVL),<sup>12</sup> valeric acid (VA),<sup>13,14</sup> and 2-methyltetrahydrofuran (MTHF).<sup>15</sup> Currently, there is much research on the cleavage of the C–O bond of LA; however, there are relatively fewer studies on the cleavage of

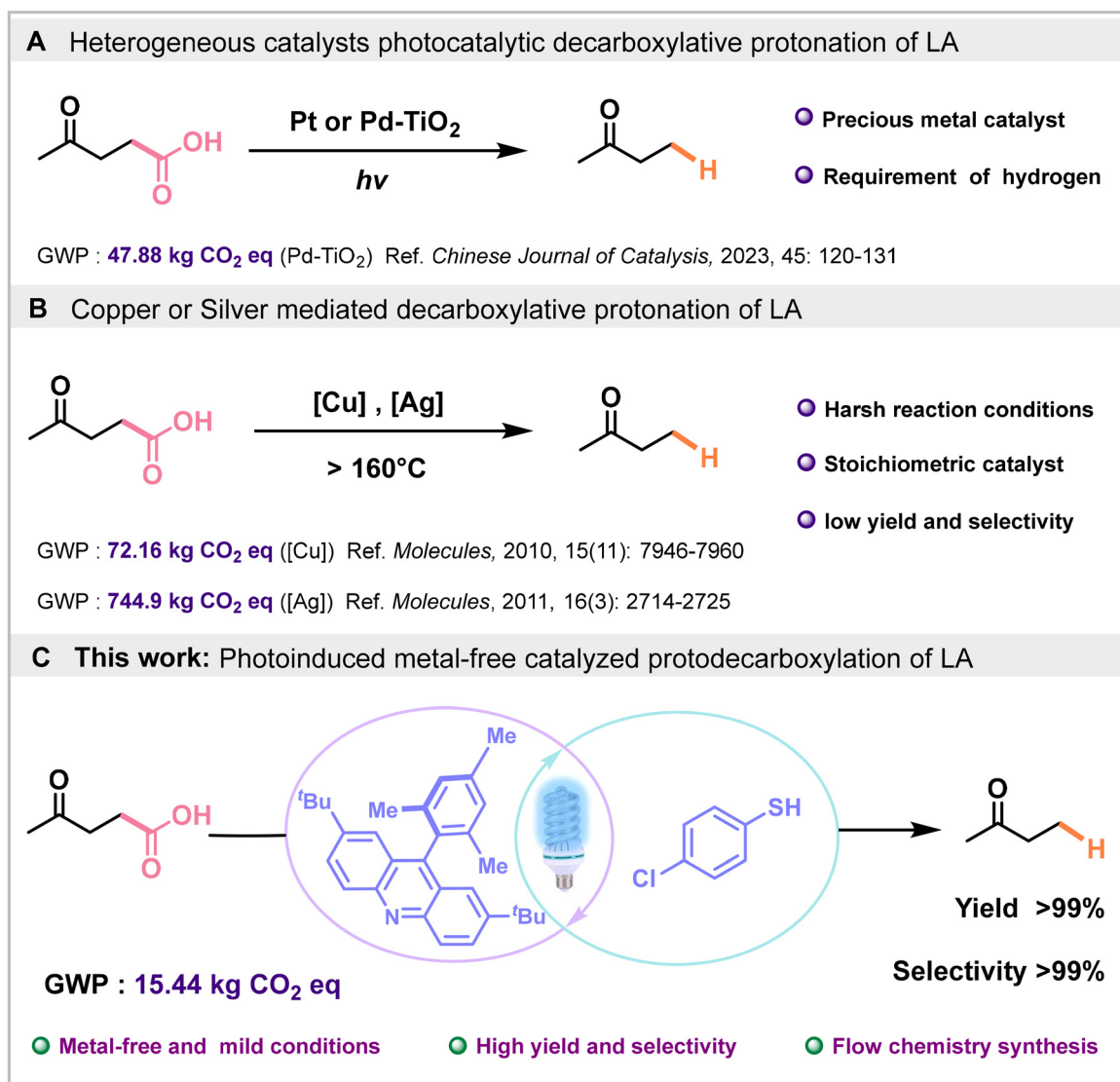
the C–C bond of LA. This is because the cleavage of the C–C bond in LA is more difficult than the C–O bond.

Methyl ethyl ketone (MEK) is a high-quality oxygen-containing low-boiling point solvent, which is widely used in industries such as medicine, coatings, dyestuffs, detergents, fragrances, and electronics.<sup>16</sup> Its molecule contains carbonyl group, which can be converted into ethyl acetate through Baeyer–Villiger oxidation,<sup>17</sup> and ethyl acetate can be further hydrolyzed to produce widely used ethanol. At the same time, MEK can also be reduced to butanol,<sup>18</sup> which is a cleaner and better fuel than ethanol.<sup>19</sup> In addition, MEK is an essential organic chemical raw material for producing chemical products such as methyl propenyl ketone, 2-heptanone, 2-butanone oxime, and 2,3-butandione.<sup>20</sup>

At present, the industrial production of MEK is mainly based on the hydration of *n*-butene to prepare *sec*-butanol and then the dehydrogenation of *sec*-butanol, while the production of *n*-butene primarily relies on petroleum cracking and pyrolysis.<sup>21</sup> Therefore, to reduce the dependence on fossil resources and meet the requirements of green chemistry, it is essential to use the biomass-based platform compound LA to prepare MEK. To date, several strategies for the decarboxylation of LA to prepare MEK have been reported. In 1983, Chum and co-workers<sup>22</sup> used Pt–TiO<sub>2</sub> as a photocatalyst to catalyze the decarboxylative protonation of LA under xenon lamp irradiation, which prepared MEK, acetic acid, acetone, and acetaldehyde in one-pot method (Scheme 1A). Unfortunately, the yield and

Key Laboratory of Precision and Intelligent Chemistry, CAS Key Laboratory of Urban Pollutant Conversion, Anhui Province Key Laboratory of Biomass Clean Energy, Department of Applied Chemistry, University of Science and Technology of China, Hefei, China. E-mail: [dengjin@ustc.edu.cn](mailto:dengjin@ustc.edu.cn)

† Electronic supplementary information (ESI) available. See DOI: <https://doi.org/10.1039/d4gc02798a>



**Scheme 1** Reaction development of decarboxylative protonation of LA.

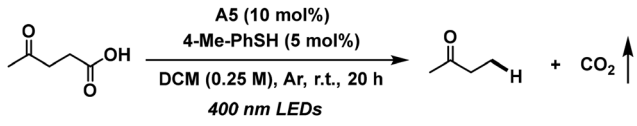
selectivity of MEK in this reaction were both low. Similarly, Wang and co-workers<sup>23</sup> reported that MEK could be obtained by photocatalytic decarboxylative protonation of LA with heterogeneous photocatalyst Pd-TiO<sub>2</sub> (Scheme 1A). Although the selectivity of MEK was increased, it also required precious metal catalyst. Moreover, this reaction required hydrogen as a source of hydrogen. Lin and co-workers<sup>24,25</sup> reported copper or silver mediated decarboxylative protonation of LA to afford MEK (Scheme 1B). Although the methods of Lin's co-workers were able to increase the yield of MEK, it required a stoichiometric catalyst and harsh reaction conditions.

Given the problems in the previous work and the acridine thiophenol synergistic catalytic system reported by our group,<sup>26</sup> we reported the efficient decarboxylative protonation of LA through a visible light-mediated proton-coupled electron transfer (PCET) process using acridine compounds and thiophenol as catalysts under mild reaction conditions

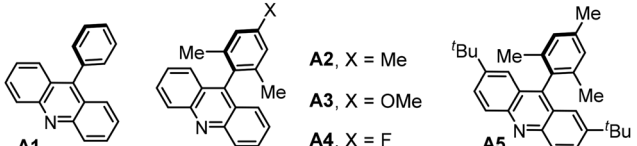
(Scheme 1C). Noteworthy features of this solution include (1) no need for any transition metal, (2) quantitative MEK yield, and (3) shortened reaction time and improved reaction efficiency through the continuous flow reactor. In addition, we also evaluated the impact of this reaction system on global warming potential (GWP) through life cycle assessment. We compared it with the carbon emissions of other methods for producing MEK from LA. The result showed that the carbon emissions of this method were relatively low.

## Results and discussion

Initially, our study selected 4-Me-PhSH (5 mol%) as the hydrogen transfer reagent with dichloromethane (DCM) as the solvent under the irradiation of 400 nm LEDs for 20 h at room temperature in N<sub>2</sub> atmosphere (Table 1). A series of acridine

**Table 1** Optimization of reaction conditions


Entry	Variation from the standard conditions	Yield (%)	Selectivity (%)
1	None	93	>99
2	A1 instead of A5	27	41
3	A2 instead of A5	62	80
4	A3 instead of A5	7	88
5	A4 instead of A5	69	93
6	Eosin Y instead of A5	0	—
7	4CzIPN instead of A5	0	—
8	Mes-Acr-MeClO <sub>4</sub> instead of A5	0	—
9	Mes-Acr-PhBF <sub>4</sub> instead of A5	0	—
10	Ir[dF(CF <sub>3</sub> )ppy] <sub>2</sub> (dtbbpy)PF <sub>6</sub> instead of A5	0	—
11	Without A5 or 400 nm LEDs	0	—
12	Without 4-Me-PhSH	<5	—
13	Without Ar	13	41



Reaction conditions: 0.5 mmol LA, 0.05 mmol photocatalyst (10 mol%), 0.025 mmol 4-Me-PhSH (5 mol%), 2.0 mL DCM (0.25 M), 400 nm LEDs (20 W), Ar, room temperature (RT), 20 h. Yield and selectivity were determined by GC with *n*-dodecane as the internal standard.

photocatalysts (10 mol%) were screened. After optimization of the conditions, the direct decarboxylative hydrogenation of LA could be effectively catalyzed utilizing photocatalyst A5 to afford MEK in 93% yield (Table 1, entry 1). The reaction provided only 27% yield of the target product when 9-phenylacridine (A1) was used as the photocatalyst (Table 1, entry 2). When the 9-phenyl of acridine was substituted with 2,4,6-trimethylphenyl (A2), the product yield increased to 62% (Table 1, entry 3). However, the addition of an electron-donating group in 9-phenyl (A3) resulted in a lower reaction yield (7% yield, Table 1, entry 4). In contrast, 9-phenyl with an electron-withdrawing group (A4) afforded the product in 69% yield (Table 1, entry 5). Additionally, when iridium-based photocatalysts such as Ir(dF(CF<sub>3</sub>)ppy)<sub>2</sub>(dtbbpy)PF<sub>6</sub> or conventional *N*-substituted acridinium-based photocatalysts such as Mes-Acr-PhBF<sub>4</sub> and Mes-Acr-MeClO<sub>4</sub> were combined with 4-Me-PhSH, the reaction failed to afford the desired product (Table 1, entries 6–10). These results indicated that conventional photocatalysts could not directly oxidize LA without bases to produce MEK. In addition, controlled experiments demonstrated that acridine photocatalyst, light source, and hydrogen atom transfer catalyst were all necessary for decarboxylative protonation of LA (Table 1, entries 11 and 12), and the yield of MEK in air was significantly reduced (13% yield, Table 1, entry 13).

After research on photocatalysts, we tested several hydrogen atom transfer catalysts to further improve reaction efficiency

(Fig. 1). The results showed that thiophenols with electron-withdrawing groups provided higher yields than 4-methyl thiophenol which bore electron-donating groups. Thiophenols bearing bulky steric hindrance groups, diphenyl sulphide, and thiol afforded lower yields in this reaction.

Based on the above research results, we screened various solvents to determine the most suitable reaction solvent. Fig. 2 showed the distribution of product in six different solvents of methanol (MeOH), *N,N*-dimethylformamide (DMF), diethyl carbonate (DEC), acetone, MEK, and dichloromethane (DCM). Only trace amounts of MEK were produced using the polar protic solvent MeOH. Similarly, when using the highly polar solvent DMF, the yield of MEK was only 16%. When the weakly polar solvent DEC was used, the yield of MEK increased to 54%. The yield and selectivity of MEK were relatively high when using the medium polar solvents DCM and acetone. Specifically, when DCM was used as the solvent, a quantitative yield of MEK was obtained with a TON (turnover number) of 10 and a TOF (turnover frequency) of 0.5 h<sup>-1</sup>. Considering that the yield of MEK exceeded 90% when acetone was used as the solvent, to facilitate the separation of the product from the reaction system and use a greener solvent than DCM, we tried to use MEK as the solvent. Fortunately, we also obtained a quantitative yield of MEK. However, in the subsequent optimization experiments, we chose to use DCM as the solvent to facilitate the calculation of MEK yield.

Next, we examined the effect of substrate concentration on the reaction results. It could be seen from the data in Fig. 3 that quantitative MEK could be obtained when the concentration of LA was lower than 0.25 mol L<sup>-1</sup>. As the concentration

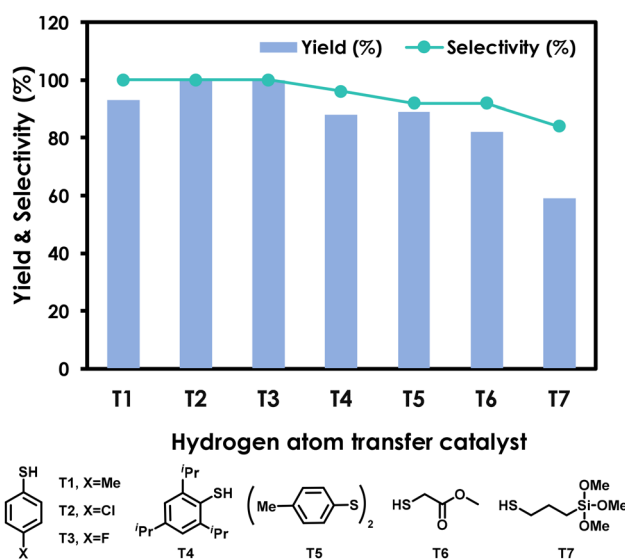


**Fig. 1** Effects of hydrogen atom transfer catalysts for decarboxylative protonation of LA. Reaction conditions: 0.5 mmol LA, 0.05 mmol 9-mesityl-2,7-di-tert-butyl-10-acridine (A5) (10 mol%), 0.025 mmol thiophenol or thiol (5 mol%), 2.0 mL DCM (0.25 M), 400 nm LEDs (20 W), Ar, room temperature (RT), 20 h. Yield and selectivity were determined by GC with *n*-dodecane as the internal standard.

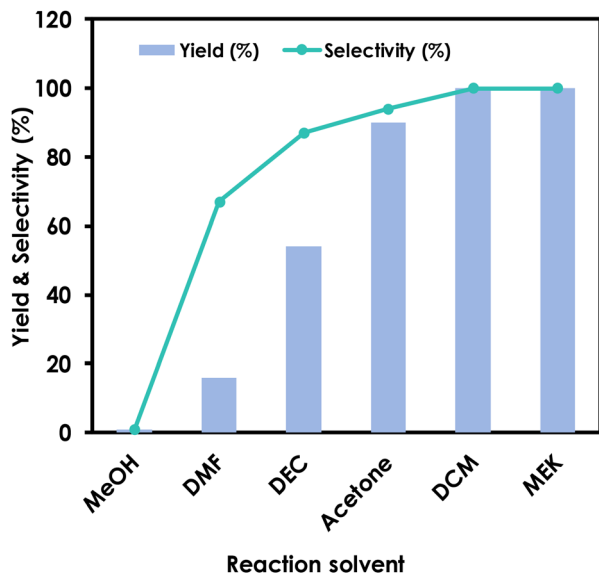


**Fig. 2** Effects of solvents for decarboxylative protonation of LA. Reaction conditions: 0.5 mmol LA, 0.05 mmol 9-mesityl-2,7-di-*tert*-butyl-10-acridine (A5) (10 mol%), 0.025 mmol 4-Cl-PhSH (5 mol%), 2.0 mL solvent (0.25 M), 400 nm LEDs (20 W), Ar, room temperature (RT), 20 h. Yield and selectivity were determined by GC with *n*-dodecane as the internal standard.

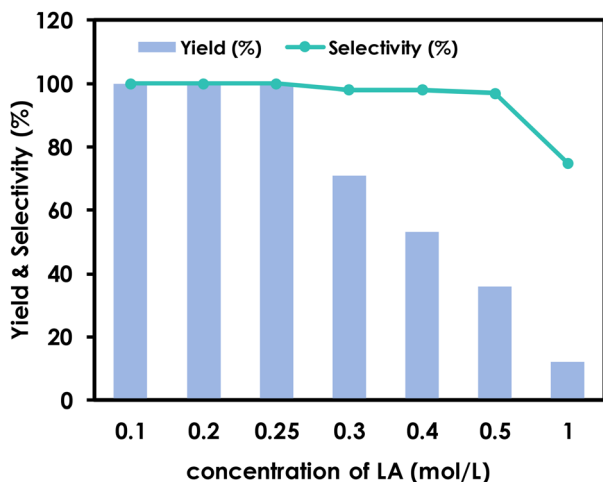


**Fig. 3** Effects of LA concentration for decarboxylative protonation of LA. Reaction conditions: 0.5 mmol LA, 0.05 mmol 9-mesityl-2,7-di-*tert*-butyl-10-acridine (A5) (10 mol%), 0.025 mmol 4-Cl-PhSH (5 mol%), *x* mL DCM (0.25 M), 400 nm LEDs (20 W), Ar, room temperature (RT), 20 h. Yield and selectivity were determined by GC with *n*-dodecane as the internal standard.

of LA was higher than 0.25 mol L<sup>-1</sup>, the reaction efficiency would decrease with the increase of LA concentration. This decline could be attributed to both a reduced conversion of LA and a lower selectivity for MEK. The diminished MEK selectivity was likely due to high LA concentration, where alkyl radical from LA decarboxylation combined with acridine radical, leading to the formation of byproducts.<sup>27</sup>

Then, to obtain the optimum amount of photocatalyst and hydrogen atom transfer reagent, we attempted to reduce the amount of catalyst based on the previously optimized conditions (Fig. 4). The results demonstrated that when the amount of photocatalyst was reduced, the yield and selectivity of the product were significantly decreased. The reduction of the amount of hydrogen atom transfer reagent had relatively less effect on the yield and selectivity of MEK. However, 5 mol% *p*-chlorothiophenol (4-Cl-PhSH) was required to obtain a quantitative yield of MEK.

To investigate the mechanism of photocatalytic reaction further, we conducted the radical trapping experiment. Only a trace amount of MEK was obtained with the addition of 3.0 equiv. 2,2,6,6-tetramethylpiperidinyloxy (TEMPO) as a free radical trap, and the decarboxylative protonation of LA was almost completely inhibited (Fig. 5A). Meanwhile the TEMPO adduct was detected by GC-MS (Fig. S2†). These results indicated that the reaction may be a free radical process.

Based on the previously reported work on photocatalytic decarboxylation of carboxylic acid,<sup>28–31</sup> we proposed a possible catalytic cycle as illustrated in Fig. 5B. Firstly, LA interacted with acridine to form a hydrogen-bonding complex, and this complex was irradiated by visible light to generate the excited state, which followed by a PCET process to produce acridine radical and carboxyl radical. Next, the carboxyl radical quickly released a molecule of carbon dioxide to form alkyl radical. Subsequently, the alkyl radical captured the hydrogen atom of 4-Cl-PhSH to afford the product MEK and thiyl radical through a hydrogen atom transfer process. Finally, both catalysts regenerated *via* the SET process from acridine radical and thiyl radical.

Continuous flow reactors have attracted much attention in the past decade due to their high mass and heat transfer efficiency, lack of amplification effects, and safer chemical processes.<sup>32</sup> Therefore, to further improve the reaction efficiency, we performed a scale-up reaction of 50 mmol using a micro-channel continuous flow photoreactor (see ESI† for more details). As mentioned in the previous solvent screening section, considering the separation problem of the product, we chose MEK as the solvent in large-scale experiments. When MEK was used as the solvent, the quantitative conversion of LA into MEK allowed for the separation and purification of MEK by distilling the reaction mixture. As shown in Fig. 6, LA and catalysts were dissolved in MEK and then entered into the 3 ml microchannel reaction plate at a 10.0 mL min<sup>-1</sup> flow rate through a peristaltic pump. Under the irradiation of 400 nm LEDs (600 mW cm<sup>-2</sup>), the reaction mixture retained 5 min in the microchannel reaction plate with the conversion of LA at 27%. The residence time was further extended (Table 2). When the residence time was 45 min, MEK was obtained in quantitative yield with a TON of 10 and a TOF of 13.3 h<sup>-1</sup>, which significantly shortened the reaction time compared with the batch reaction, which required 20 h of reaction to afford a quantitative yield of MEK. This was due to using a flow reactor device, which allowed for a larger illumination area and liquid–liquid interfacial area.<sup>33</sup>

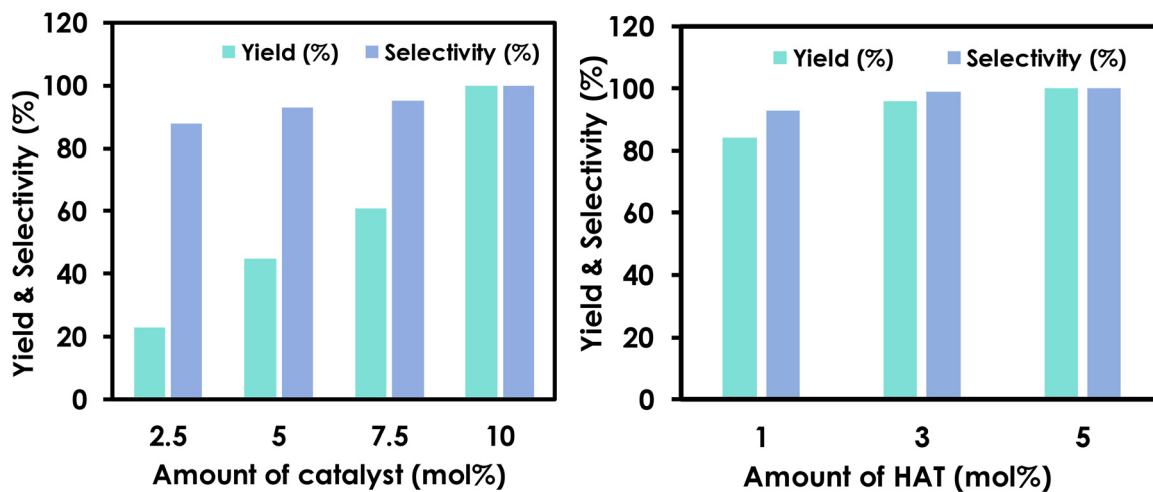


Fig. 4 Effects of the amount of photocatalyst and hydrogen atom transfer reagent for decarboxylative protonation of LA.

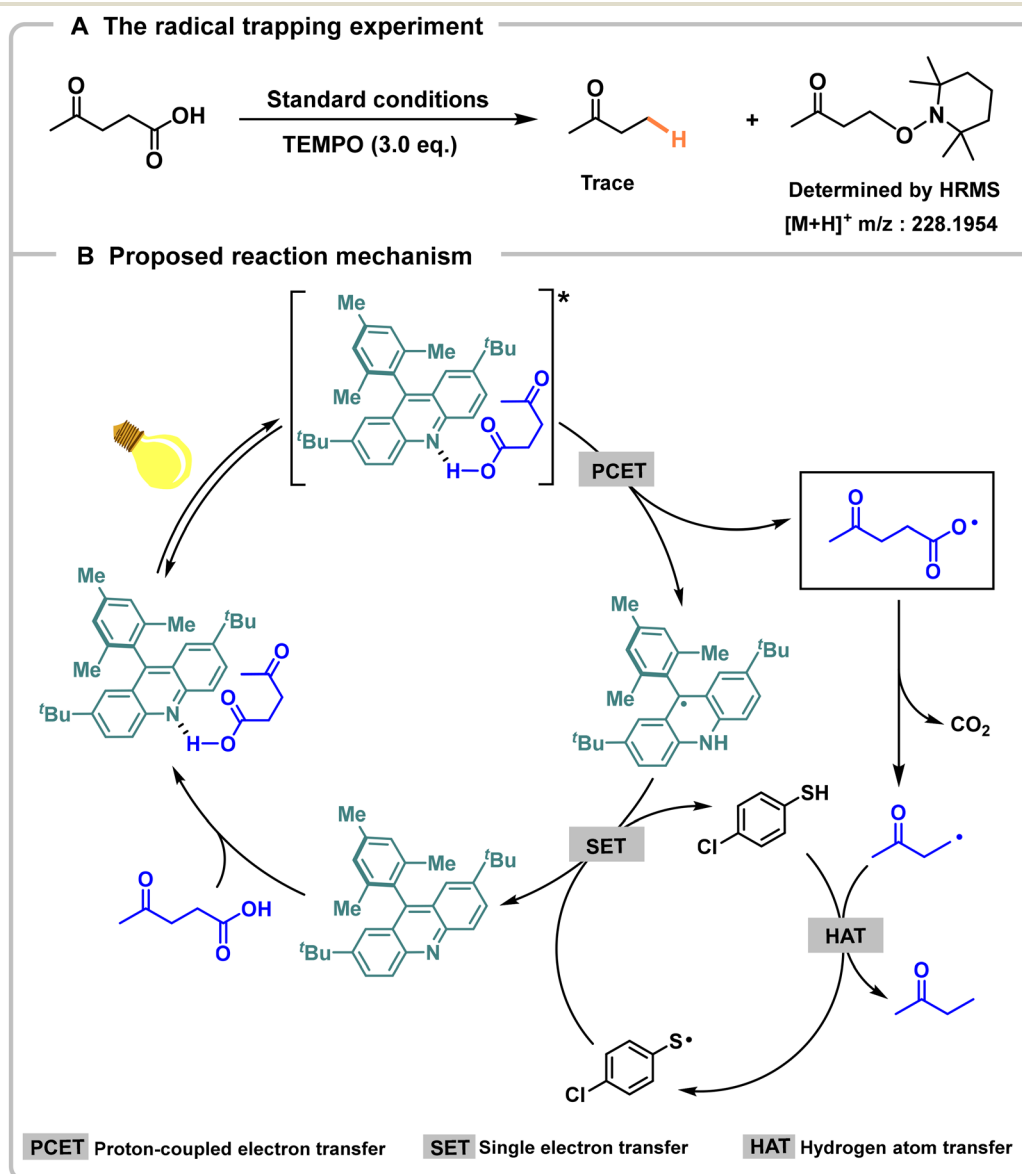


Fig. 5 Reaction path and mechanism studies.

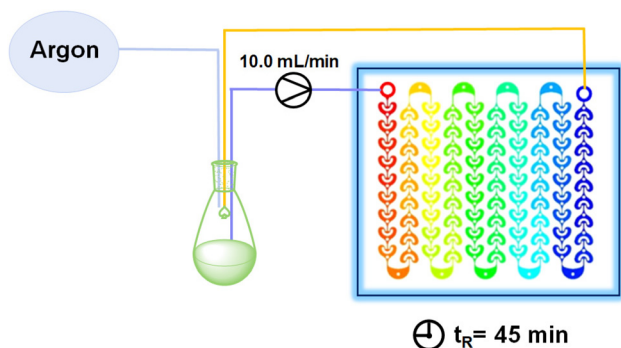


Fig. 6 Continuous synthesis of MEK from the decarboxylative protonation of LA.

Table 2 Effects of residence time on continuous flow reactions

Entry	Residence time (min)	Conversion (%)
1	5	27
2	15	61
3	30	93
4	45	>99

Reaction conditions: 50 mmol LA, 5 mmol 9-mesityl-2,7-di-*tert*-butyl-10-acridine (A5) (10 mol%), 2.5 mmol 4-Cl-PhSH (5 mol%), 200.0 mL MEK (0.25 M), 400 nm LEDs, Ar, room temperature (RT). Conversion was determined by GC with *n*-dodecane as the internal standard. There were only MEK peak, internal standard peak, and LA peak in the gas chromatogram.

## Life cycle assessment

With complete and optimized experimental data, a life cycle assessment (LCA) was conducted to evaluate the impact of various MEK production approaches *via* LA on the GWP.

LCA is an analytical tool in the ISO 14040 and ISO 14044 series of standards for assessing the environmental impact of a product or service. An accurate assessment should be as comprehensive as possible, including the sum of all material inputs and outputs, energy consumption, and other process attributes such as reprocessing, transportation, and waste management procedures.<sup>34,35</sup>

In recent years, several life cycle assessments have emerged in the field of chemistry, with a focus on demonstrating the benefits of applying biobased feedstocks,<sup>36,37</sup> alternative synthetic methods,<sup>38,39</sup> and innovative processes.<sup>40</sup> Nevertheless, many of these new researches have been conducted only at an early stage of development, for example, at the laboratory scale or during process simulations. The purpose is to identify critical aspects of improved upscaling or to illustrate the justification for selecting one of several approaches.<sup>41,42</sup>

This LCA model aimed to compare the GWP data of different methods of producing MEK from LA. The functional unit of the study was the production of 1 kg of MEK. The system boundary of this LCA was “gate-to-gate,” including all processes from the factory receiving LA to the factory gate

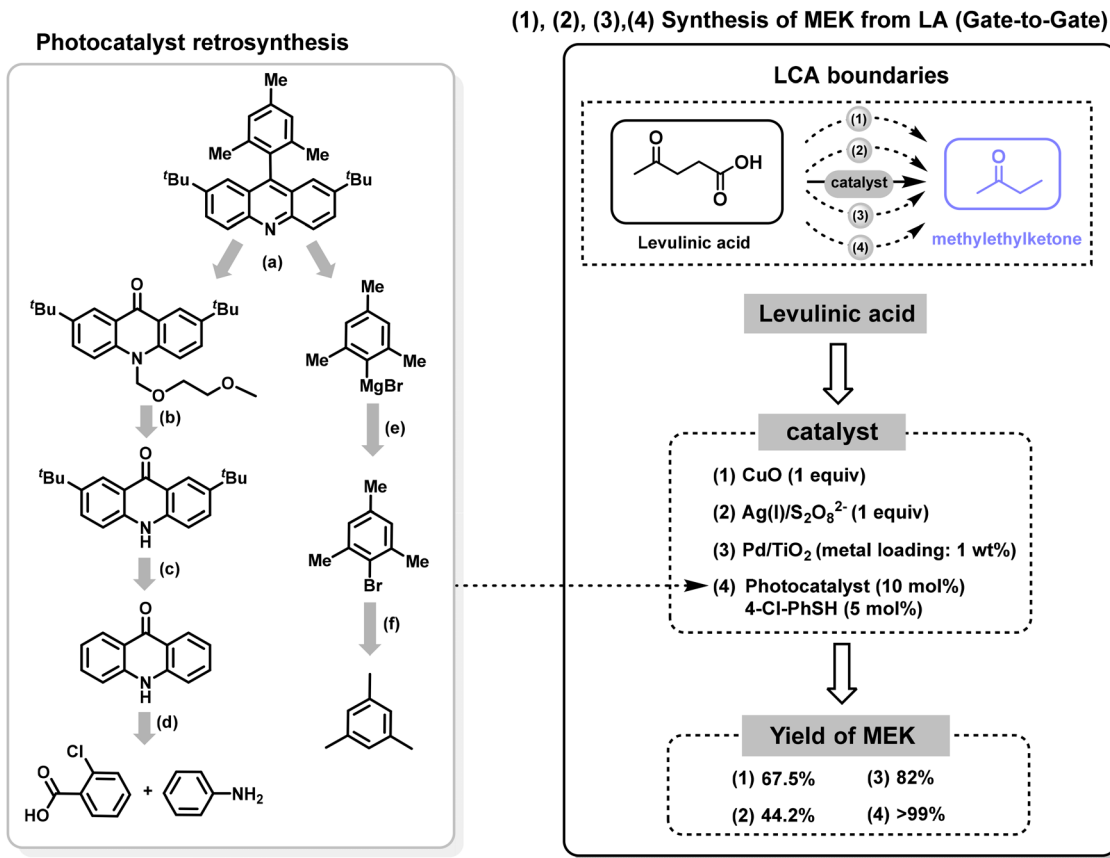
where MEK was synthesized (Fig. S5†). In this case, the applied catalysts were modelled from cradle to gate to demonstrate the impact of their use in this reaction on GWP.

The life cycle inventory (LCI) included four different methods for the decarboxylation of LA to MEK, which were Scenario (1) copper mediated decarboxylative protonation of LA,<sup>24</sup> Scenario (2) silver mediated decarboxylative protonation of LA,<sup>25</sup> Scenario (3) Pd-TiO<sub>2</sub> catalyzed decarboxylative protonation of LA,<sup>23</sup> Scenario (4) photoinduced metal-free catalyzed proto-decarboxylation of LA (Scheme 2). Herein, detailed inventory data came from experimental data (foreground system), the Ecoinvent v3.8 database (background system), and some published literature.<sup>43</sup> The entire procedure of the decarboxylation reaction and catalyst synthesis route was modelled in openLCA software, and the GWP was calculated using the CML-IA baseline method.

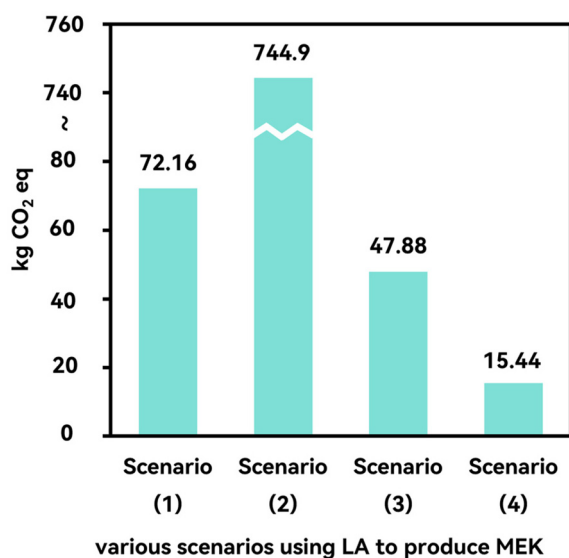
The process of converting LA to MEK was accomplished by heating or lighting, thus, LA, catalyst, and heat or light were all inputs. Among them, the GWP values of the catalysts used in Scenarios (1–3) were from the Ecoinvent v3.8 database. To evaluate the carbon footprint of the catalysts used in Scenario (4), a reasonable retrosynthetic route was designed based on reports in the literature to find simpler precursor compounds that might be available in the database (Scheme 2).<sup>26,44–47</sup> Firstly, 2,7-di-*tert*-butyl-9-mesitylacridine (A5) was synthesized from 2,7-di-*tert*-butyl-10-((2-methoxyethoxy)methyl)acridin-9 (10*H*)-one and mesitylmagnesium bromide, as illustrated in Scheme 2.<sup>26</sup> Subsequently, further retrosynthetic analysis was carried out according to the synthesis methods in the literature, which were finally derived from 2-chlorobenzoic acid, aniline, and 1,3,5-trimethyl-benzene respectively.

Fig. 7 presented the GWP results for different scenarios of MEK production from LA. The data showed that our method had the lowest GWP value over the “gate-to-gate” life cycle of producing 1 kg MEK. The GWP value of Scenario (2) was 744.9 kg CO<sub>2</sub> eq., which was significantly higher than the other three scenarios. This was attributed to the use of the equivalent precious metal silver and lower MEK yield in this method. Although Scenario (3) also utilized the precious metal Pd, its quantity was at catalytic levels (approximately 0.3 mol%), resulting in a lower GWP value compared to Scenario (2). Scenario (1) showed a GWP value of 72.16 kg CO<sub>2</sub> eq. Despite employing the equivalent catalyst CuO, its lower carbon emissions during CuO production lead to a considerably lower GWP value than Scenario (2). In our method (Scenario (4)), catalytic amounts of metal-free catalyst were utilized, and LA was converted entirely into MEK. Thus, our proposed method of producing MEK from LA had the least carbon footprint.

It was worth noting that the GWP value over the “cradle-to-gate” life cycle of producing 1 kg MEK from fossil resources was only 1.88 kg CO<sub>2</sub> eq. (data comes from Ecoinvent v3.8 database, evaluation method was CML-IA baseline, Table S1†). Assuming that MEK was ultimately burned to produce CO<sub>2</sub>, the total carbon emissions from “cradle-to-grave” for petroleum-based MEK was 4.32 kg CO<sub>2</sub> eq. For “cradle-to-gate”



**Scheme 2** The system boundary of LCA study on MEK production from LA: gate-to-gate comparative assessment including Scenario (1) copper mediated decarboxylative protonation of LA, Scenario (2) silver mediated decarboxylative protonation of LA, Scenario (3) Pd-TiO<sub>2</sub> catalyzed decarboxylative protonation of LA, Scenario (4) photoinduced metal-free catalyzed protodecarboxylation of LA. Reaction conditions: (a) in THF, Ar, 24 h, 62%;<sup>26</sup> (b) in DMF, Ar, 12 h, 50%;<sup>44</sup> (c) in CH<sub>2</sub>Cl<sub>2</sub>, AlCl<sub>3</sub>, 24 h, 100%;<sup>45</sup> (d) in water, sodium hydroxide, 4.0 h, 95%;<sup>46</sup> (e) in THF, Mg, anhydrous, 100%; (f) in water, hydrogen bromide; dihydrogen peroxide, 24 h, 98%.<sup>47</sup>



**Fig. 7** Global Warming Potential (GWP) results for four different scenarios of MEK production from LA.

life cycle of producing 1 kg bio-based LA, the lowest GWP value was 2.40 kg CO<sub>2</sub> eq.,<sup>48</sup> and making 1 kg MEK from bio-based LA resulted in a minimum “gate-to-gate” GWP value of 15.44 kg CO<sub>2</sub> eq. Therefore, the lowest total “cradle-to-grave” carbon emissions for bio-based MEK were 17.84 kg CO<sub>2</sub> eq., higher than that for petroleum-based MEK. These results indicated that bio-based products did not always have the expected positive environmental impact. Furthermore, the high molecular weight and substantial dosage of acridine photocatalysts, coupled with the cost of hydrogen transfer agents, resulted in significant economic expenses for this process. Therefore, to lower the carbon emissions and economic costs of bio-based MEK production, it is essential to develop more sustainable catalyst synthesis methods and implement catalyst recycling.

## Conclusions

This study described a synergistic catalytic system of acridine and thiophenol for the photocatalytic decarboxylation of LA to produce MEK using metal-free catalysts. The process achieved high selectivity and yield under mild conditions by employing

acridine derivatives as the photosensitizer and thiophenol as the hydrogen transfer agent. Using a microchannel continuous flow photoreactor significantly shortened the reaction time and improved the reaction efficiency. Life cycle assessment showed that this method had a lower carbon footprint than other methods of producing MEK from LA. This work provided a promising approach for producing MEK from biomass-derived LA, contributing to reducing dependence on fossil resources and supporting green chemistry initiatives. Further research could focus on improving the scalability and reducing the carbon footprint to make the process more competitive with traditional MEK production methods.

## Author contributions

Meng-Xiang Shen: data curation, investigation, formal analysis, and writing – original draft. Chen-Qiang Deng: writing – review and editing. Jie Yang: contributed to life-cycle assessment. Jin Deng: conceptualization, methodology, project administration, resources, supervision, and review.

## Data availability

The data supporting this article have been included as part of the ESI.†

## Conflicts of interest

There are no conflicts to declare.

## Acknowledgements

The authors thank Anhui Kemi Machinery Technology Co., Ltd, for providing the photoreactor equipment that benefited our ability to conduct this study. The authors also thank Anhui Kexin Microflow Chemical Technology Co., Ltd, for providing the continuous flow photoreactor that benefited our ability to conduct scale up production. This work was supported by the National Natural Science Foundation of China (22478374 and 22279125).

## References

- 1 A. Corma, S. Iborra and A. Velty, *Chem. Rev.*, 2007, **107**, 2411–2502.
- 2 D. Sun, Y. Yamada, S. Sato and W. Ueda, *Appl. Catal., B*, 2016, **193**, 75–92.
- 3 A. Villa, N. Dimitratos, C. E. Chan-Thaw, C. Hammond, L. Prati and G. J. Hutchings, *Acc. Chem. Res.*, 2015, **48**, 1403–1412.
- 4 G. Dodekatos, S. Schünemann and H. Tüysüz, *ACS Catal.*, 2018, **8**, 6301–6333.
- 5 X. Kong, R. Zheng, Y. Zhu, G. Ding, Y. Zhu and Y.-W. Li, *Green Chem.*, 2015, **17**, 2504–2514.
- 6 G. W. Huber, S. Iborra and A. Corma, *Chem. Rev.*, 2006, **106**, 4044–4098.
- 7 M. J. Climent, A. Corma and S. Iborra, *Green Chem.*, 2014, **16**, 516.
- 8 W. Luo, M. Sankar, A. M. Beale, Q. He, C. J. Kiely, P. C. A. Bruijninx and B. M. Weckhuysen, *Nat. Commun.*, 2015, **6**, 6540.
- 9 X.-L. Du, L. He, S. Zhao, Y.-M. Liu, Y. Cao, H.-Y. He and K.-N. Fan, *Angew. Chem., Int. Ed.*, 2011, **50**, 7815–7819.
- 10 D. Lai, L. Deng, Q. Guo and Y. Fu, *Energy Environ. Sci.*, 2011, **4**, 3552–3557.
- 11 W.-P. Xu, X.-F. Chen, H.-J. Guo, H.-L. Li, H.-R. Zhang, L. Xiong and X.-D. Chen, *J. Chem. Technol. Biotechnol.*, 2021, **96**, 3009–3024.
- 12 B. Zada, R. Zhu, B. Wang, J. Liu, J. Deng and Y. Fu, *Green Chem.*, 2020, **22**, 3427–3432.
- 13 L. Gan, C. Deng and J. Deng, *Green Chem.*, 2022, **24**, 3143–3151.
- 14 J. Zhou, R. Zhu, J. Deng and Y. Fu, *Green Chem.*, 2018, **20**, 3974–3980.
- 15 L. Gan and J. Deng, *Green Chem.*, 2023, **25**, 4536–4543.
- 16 D. Song, *Ind. Eng. Chem. Res.*, 2016, **55**, 11664–11671.
- 17 W. D. Emmons and G. B. Lucas, *J. Am. Chem. Soc.*, 1955, **77**, 2287–2288.
- 18 Z. Lou, X. Chen, L. Tian, M. Qiao, K. Fan, H. He, X. Zhang and B. Zong, *J. Mol. Catal. A: Chem.*, 2010, **326**, 113–120.
- 19 N. Qureshi, B. C. Saha and M. A. Cotta, *Biomass Bioenergy*, 2008, **32**, 176–183.
- 20 M. C. Álvarez-Galván, V. A. de la Peña O'Shea, G. Arzamendi, B. Pawelec, L. M. Gandía and J. L. G. Fierro, *Appl. Catal., B*, 2009, **92**, 445–453.
- 21 L. Torres-Vinces, G. Contreras-Zarazua, B. Huerta-Rosas, E. Sánchez-Ramírez and J. G. Segovia-Hernández, *Chem. Eng. Technol.*, 2020, **43**, 1433–1441.
- 22 H. L. Chum, M. Ratcliff, F. L. Posey, J. A. Turner and A. J. Nozik, *J. Phys. Chem.*, 1983, **87**, 3089–3093.
- 23 Z. Huang, Y. Yang, J. Mu, G. Li, J. Han, P. Ren, J. Zhang, N. Luo, K.-L. Han and F. Wang, *Chin. J. Catal.*, 2023, **45**, 120–131.
- 24 Y. Gong, L. Lin, J. Shi and S. Liu, *Molecules*, 2010, **15**, 7946–7960.
- 25 Y. Gong and L. Lin, *Molecules*, 2011, **16**, 2714–2725.
- 26 C.-Q. Deng, Y. Xu, J.-H. Luo, G.-Z. Wang, J. Deng and Y. Fu, *Chem Catal.*, 2024, **4**, 100899.
- 27 K. A. Zhilyaev, D. L. Lipilin, M. D. Kosobokov, A. I. Samigullina and A. D. Dilman, *Adv. Synth. Catal.*, 2022, **364**, 3295–3301.
- 28 V. T. Nguyen, V. D. Nguyen, G. C. Haug, H. T. Dang, S. Jin, Z. Li, C. Flores-Hansen, B. S. Benavides, H. D. Arman and O. V. Larionov, *ACS Catal.*, 2019, **9**, 9485–9498.
- 29 V. D. Nguyen, G. C. Haug, S. G. Greco, R. Trevino, G. B. Karki, H. D. Arman and O. V. Larionov, *Angew. Chem., Int. Ed.*, 2022, **61**, e202210525.

- 30 H. T. Dang, V. D. Nguyen, G. C. Haug, H. D. Arman and O. V. Larionov, *JACS Au*, 2023, **3**, 813–822.
- 31 J. D. Griffin, M. A. Zeller and D. A. Nicewicz, *J. Am. Chem. Soc.*, 2015, **137**, 11340–11348.
- 32 T. Gao, J. Zhao, H. Sun, J. Li, C. Ma and Q. Meng, *Org. Process Res. Dev.*, 2024, **28**, 1464–1473.
- 33 N. Li, Y. Ning, X. Wu, J. Xie, W. Li and C. Zhu, *Chem. Sci.*, 2021, **12**, 5505–5510.
- 34 V. Isoni, D. Kumbang, P. N. Sharratt and H. H. Khoo, *J. Environ. Manage.*, 2018, **214**, 267–275.
- 35 D. Kralisch, D. Ott and D. Gericke, *Green Chem.*, 2014, **17**, 123–145.
- 36 R. Mazzoni, C. Cesari, V. Zanotti, C. Lucarelli, T. Tabanelli, F. Puzzo, F. Passarini, E. Neri, G. Marani, R. Prati, F. Viganò, A. Conversano and F. Cavani, *ACS Sustainable Chem. Eng.*, 2019, **7**, 224–237.
- 37 H. H. Khoo, W. L. Ee and V. Isoni, *Green Chem.*, 2016, **18**, 1912–1922.
- 38 M. A. F. Delgove, A.-B. Laurent, J. M. Woodley, S. M. A. De Wildeman, K. V. Bernaerts and Y. van der Meer, *ChemSusChem*, 2019, **12**, 1349–1360.
- 39 Z. Wang, Z. Li, T. Lei, M. Yang, T. Qi, L. Lin, X. Xin, A. Ajayebi, Y. Yang, X. He and X. Yan, *Appl. Energy*, 2016, **183**, 170–181.
- 40 C. Koroneos, A. Dompros, G. Roumbas and N. Moussiopoulos, *Int. J. Hydrogen Energy*, 2004, **29**, 1443–1450.
- 41 R. Arvidsson, A.-M. Tillman, B. A. Sandén, M. Janssen, A. Nordelöf, D. Kushnir and S. Molander, *J. Ind. Ecol.*, 2018, **22**, 1286–1294.
- 42 H. H. Khoo, L. L. Wong, J. Tan, V. Isoni and P. Sharratt, *Resour., Conserv. Recycl.*, 2015, **95**, 174–182.
- 43 P. Nuss and M. J. Eckelman, *PLoS One*, 2014, **9**, e101298.
- 44 T. Kanetomo, K. Ichihashi, M. Enomoto and T. Ishida, *Org. Lett.*, 2019, **21**, 3909–3912.
- 45 K. Yamamoto and S. Higashibayashi, *Chem. – Eur. J.*, 2016, **22**, 663–671.
- 46 S. Xu, J. Li, P. Cai, X. Liu, B. Liu and X. Wang, *J. Am. Chem. Soc.*, 2021, **143**, 19769–19777.
- 47 A. Podgoršek, S. Stavber, M. Zupan and J. Iskra, *Tetrahedron*, 2009, **65**, 4429–4439.
- 48 J. Yang, T. Gong, C. Li, H. Xu, S. Yu, J. Deng and Y. Fu, *Carbon Neutrality*, 2023, **2**, 17.